ARTICLE

Citrate-Capped Gold Nanoparticles as Colorimetric Reagent for Copper(II) Ions

Alan Rodelle M. Salcedo* and Fortunato B. Sevilla III

Research Center for the Natural and Applied Sciences
University of Santo Tomas, España, Manila, Philippines

Citrate-capped gold nanoparticles were prepared by chemical reduction of $HAuCl_4$ using citrate as the reducing agent and stabilizer. The synthesized nanoparticles showed an intense localized surface plasmon resonance absorption band at 520nm. Uniformly distributed spherical gold nanoparticles with average particle diameter size of 12.2±1.65nm were verified through Transmission Electron Microscopy (TEM) analysis. The stability of the gold nanoparticles was affected by pH and Cu^{2+}. Aggregates are formed at pH <3 due to surface charge neutralization of the citrate-capped gold nanoparticles. With Cu^{2+}, aggregation is being initiated at a certain concentration. Visual observations, UV-Vis spectroscopy and TEM analysis were used to characterize the aggregated system. At optimum parameters (i.e., wavelength, reaction time, and pH), a calibration curve for Cu^{2+} determination was constructed. The calibration curve has good linearity (r^2=0.9822) and sensitivity of 0.0036 A.U./mM for the linear range from 2.5mM to 100mM. Reproducible absorbance readings (r.s.d.= 1.56-6.15%, n=6) for the linear concentration range of 2.5mM to 100mM were obtained. The detection limit for Cu^{2+} determination method is 5.0 mM.

*Corresponding author
Email Address: alanx3@yahoo.com
Submitted: August 17, 2012
Revised: March 13, 2013
Accepted: March 14, 2013
Published: April 19, 2013
Editor-in-charge: Eduardo A. Padlan

KEYWORDS

gold nanoparticles, citrate reduction method, localized surface plasmon resonance, copper determination, aggregation

INTRODUCTION

Metal nanomaterials such as gold nanoparticles have found wide application in chemical analysis due to their unique optical and electrical properties. These properties of gold nanoparticles are determined by their size, shape, composition and structure. An accurate control of any one of these parameters allows the determination of the final properties of the gold nanoparticles (Aryal et al. 2007). The interesting optical properties of gold nanoparticles are due to their localized surface plasmon resonance (LSPR), which is caused by the collective oscillations of surface electrons induced by visible light and is manifested by an absorption band in the visible region of the optical spectrum (Sarkar et al. 2008, Ye et al. 2008, Wang and Ma 2009).

In solutions, gold nanoparticles tend to be fairly unstable and aggregate, thereby losing their important properties. For this reason, special precautions have to be taken to avoid their aggregation or precipitation. The most common strategy is the use of stabilizers or protective capping agents, which not only prevents their aggregation, but also results in functionalized particles (Luo 2007). Among the variety of stabilizers and protective capping agents for gold nanoparticles, the one commonly used is citrate, which stabilizes the gold nanoparticles through mutual electrostatic repulsion between neighboring gold nanoparticles; this occurs as a result of the negative surface charge of the citrate layer (Brewer et al. 2005, Sugunan and Dutta 2005).

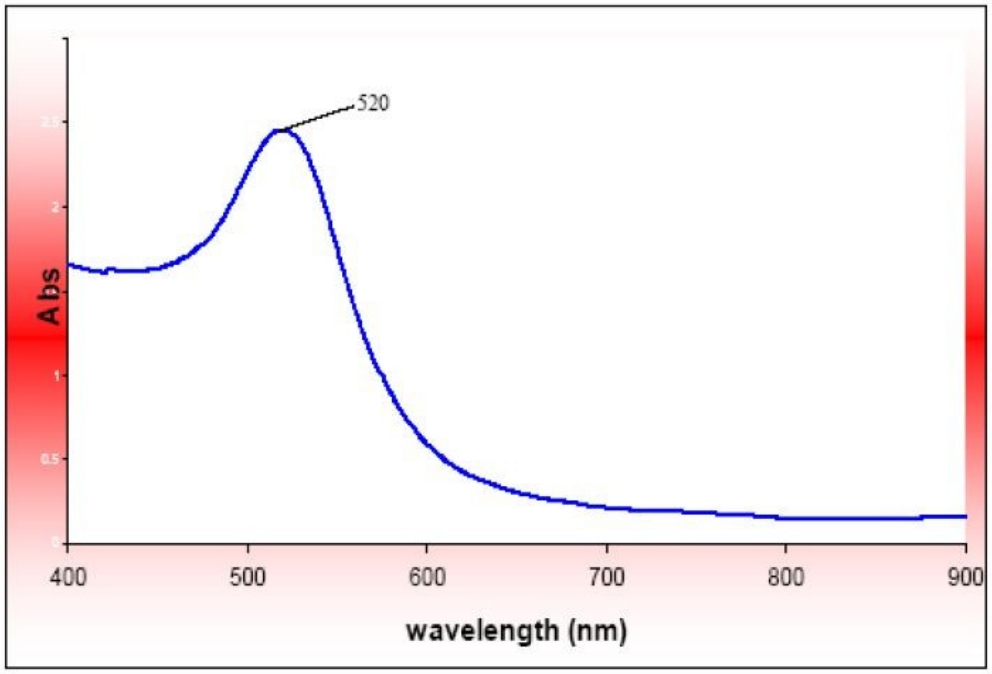

Figure 1. UV-Vis Spectrum of the citrate-capped gold nanoparticles.

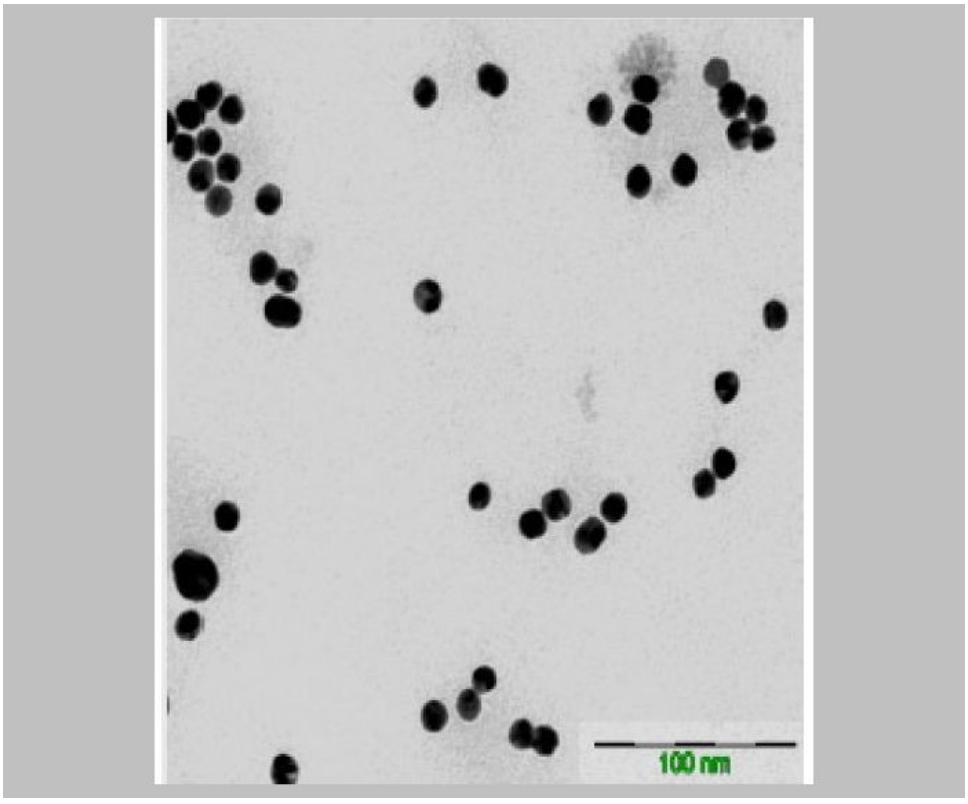

Figure 2. TEM micrograph of the citrate-capped gold nanoparticles.

Applications of gold nanoparticles as colorimetric sensors are usually based on detecting the shifts in surface plasmon resonance peak, due to either the change in the dielectric constant around the nanoparticles as a result of adsorption of analyte molecules, or to the analyte-induced agglomeration of the nanoparticles. Both of these effects rely on the selectivity provided by the functionalized capping agents, highlighting the significance of the chemical methods of synthesis and stabilization of these nanoparticles for use as solution-based sensors (Sugunan et al. 2005).

Gold nanoparticles as colorimetric sensor or probe have been widely used for several analytes such as heavy metal ions (Huang and Chang 2006, Kim et al. 2001, Lee et al. 2007, Liu and Lu 2003, Sugunan et al. 2005, Yoosaf et al. 2007), oxoanion (Kubo et al. 2005), flouride ion (Watanabe et al. 2005), hydrogen peroxide (Wu et al. 2007), organophosphates (Simonian et al. 2005), and biomolecules (Kattumuri et al. 2006, Liang et al. 2004, Rho et al. 2008, Sun et al. 2007). For example, Liu and Lu (2003) used DNA-directed assembly of gold nanoparticles as colorimetric biosensor for Pb(II). The sensor has tunable Pb(II) detection range between 100 nM and 4 μM. Sugunan et al. (2005) developed a colorimetric sensor for Cu^{2+} and Zn^{2+} based on gold nanoparticles capped with chitosan. The ability of chitosan to chelate heavy metal ions was effectively used for the detection of Cu^{2+} and Zn^{2+}. A DNA-hybridized gold nanoparticle probes were also used to detect Hg^{2+} in aqueous media (Lee et al. 2007). The colorimetric response of the gold nanoparticles solution from purple-to-red color change

was caused by the formation of thymidine-Hg^{2+}-thymidine coordination complexes. Hydrogen peroxide was also detected based on the aggregation of gold nanoparticles where the aggregation was induced by azoaniline liberated from the oxidation of *o*-phenylenediamine by hydrogen peroxide in the presence of horseradish peroxidase (Wu et al. 2007). Using this sensor, hydrogen peroxide can be accurately determined down to concentration levels of 1.3×10^{-6} M. Aslan et al. (2004) have reported the sensing of glucose through the aggregation and dissociation of 20-nm gold nanoparticles and changes in the plasmon absorption induced by glucose. The described colorimetric method proposed potential monitoring of µM glucose levels in different physiological fluids, such as tears, blood and urine.

In this study, the feasibility of using citrate-capped gold nanoparticles as a colorimetric reagent for copper(II) ions was investigated. The detection strategies were based on the color change that originate from the analyte-directed aggregation of gold nanoparticles. Interaction of copper(II) ions with the citrate on the surface of the nanoparticles could form linkages among nanoparticles with Cu(II) ions acting as bridges, or compete for the binding site of the citrate and completely removing it from the surface of the gold nanoparticles, thereby causing aggregation of the nanoparticles.

MATERIALS AND METHODS

Chemicals

All chemicals used were of analytical reagent (AR) grade and were used as received without further purification. Hydrogen tetrachloroaurate ($HAuCl_4 \cdot 3H_2O$, ≥ 49%), L-glutathione reduced (≥ 99%), and sodium citrate dihydrate were purchased from Sigma-Aldrich. All glasswares were cleaned with freshly prepared 3:1 HCl/HNO_3 (aqua regia), then rinsed thoroughly with deionized water and ovendried prior to use. Deionized water (Janija Trading) was used to prepare all solutions in this study.

For the interference study, 2.5 and 0.25 mM of the metal ion solutions were prepared by serial dilution from a 1.0 M metal ion stock solutions. The solutions were then stored in an amber bottle.

Instrumentation

UV-Vis absorbance spectra were collected using a double beam UV-Vis spectrophotometer (Perkin Elmer Lambda 35) equipped with deuterium and tungsten lamp, 2.00 nm fixed slit width, UVWINLAB v.2.85 software and operating at a maximum scan rate of 240 nm/min. Disposable UV-cuvettes

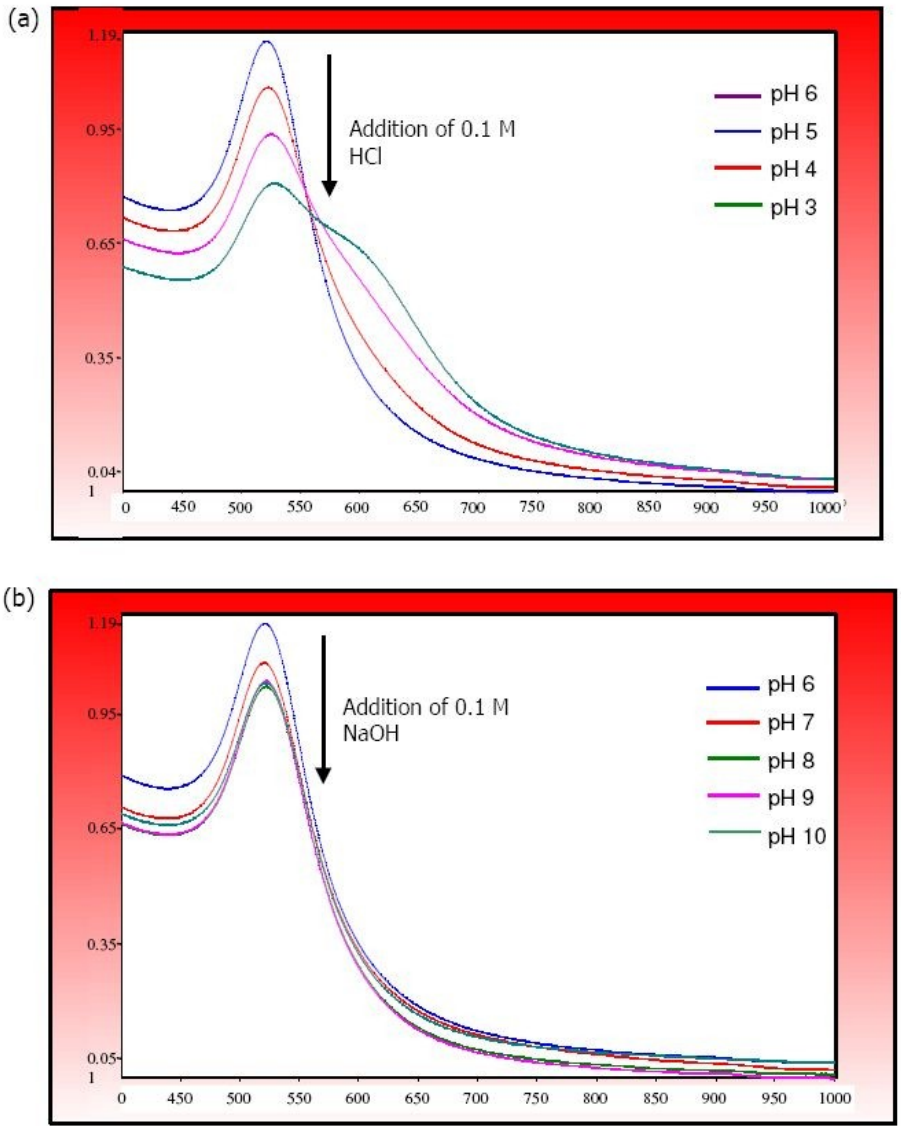

Figure 3. UV-Vis spectral evolution of the citrate-capped gold nanoparticles upon progressive addition of (a) 0.1M HCl and (b) 0.1M NaOH

(BrandTech) with 10mm-pathlength were used as sample holder for all UV-Vis analysis. Transmission Electron Microscopy (TEM) analysis was carried out with a ZEISS LIBRA®120 PLUS transmission electron microscope operated at an accelerating voltage of 120 kV. Samples were prepared by dropcasting 5 µL on a 200 mesh Formvar-coated copper grid and allowing it to dry at room temperature. Measurements of pH were employed using a Metrohm 691 pH meter which was calibrated with standard phosphate buffer solution (pH 4 and 10). Photographs of the samples and instruments were taken using a Canon PowerShot A720 digital camera.

Synthesis of Citrate-Capped Gold Nanoparticles

Citrate-capped gold nanoparticles were synthesized according to the method proposed by Rho et al. (2008). Fifty mL of 1.0mM $HAuCl_4$ solution were heated in an oil bath with vigorous stirring in a round bottom flask equipped with a condenser. Upon boiling, 5 mL of 38.8mM sodium citrate solution were rapidly added to the vortex of the solution. A transition of color was immediately observed from pale yellow to dull blue to wine red. The solution was further boiled for 30 minutes and then cooled with stirring to room temperature. It was then filtered and kept in a refrigerator using a glass amber bottle container. The pH of the gold nanoparticles solutions was measured and adjusted to desired values with 0.1M HCl, or 0.1M NaOH. The gold nanoparticles solution was further characterized by UV-Vis spectroscopy and TEM.

Assay of Copper(II) Ion

In order to demonstrate the effect of Cu^{2+} ions on the aggregation of gold nanoparticles, 500µL portions of different concentrations of Cu^{2+} (2.5mM, 5.0mM, 10.0mM, 25.0mM, 50.0mM, and 100mM) were added individually to 500µL of gold nanoparticle solution and the resulting mixtures were then allowed to react for 6 min. Subsequently, the absorbance changes at 700 nm were monitored. The pH values of the gold nanoparticle solutions were varied using 0.1M HCl, or 0.1M NaOH, from pH 4 to pH 10 to investigate the effect of pH on the aggregation.

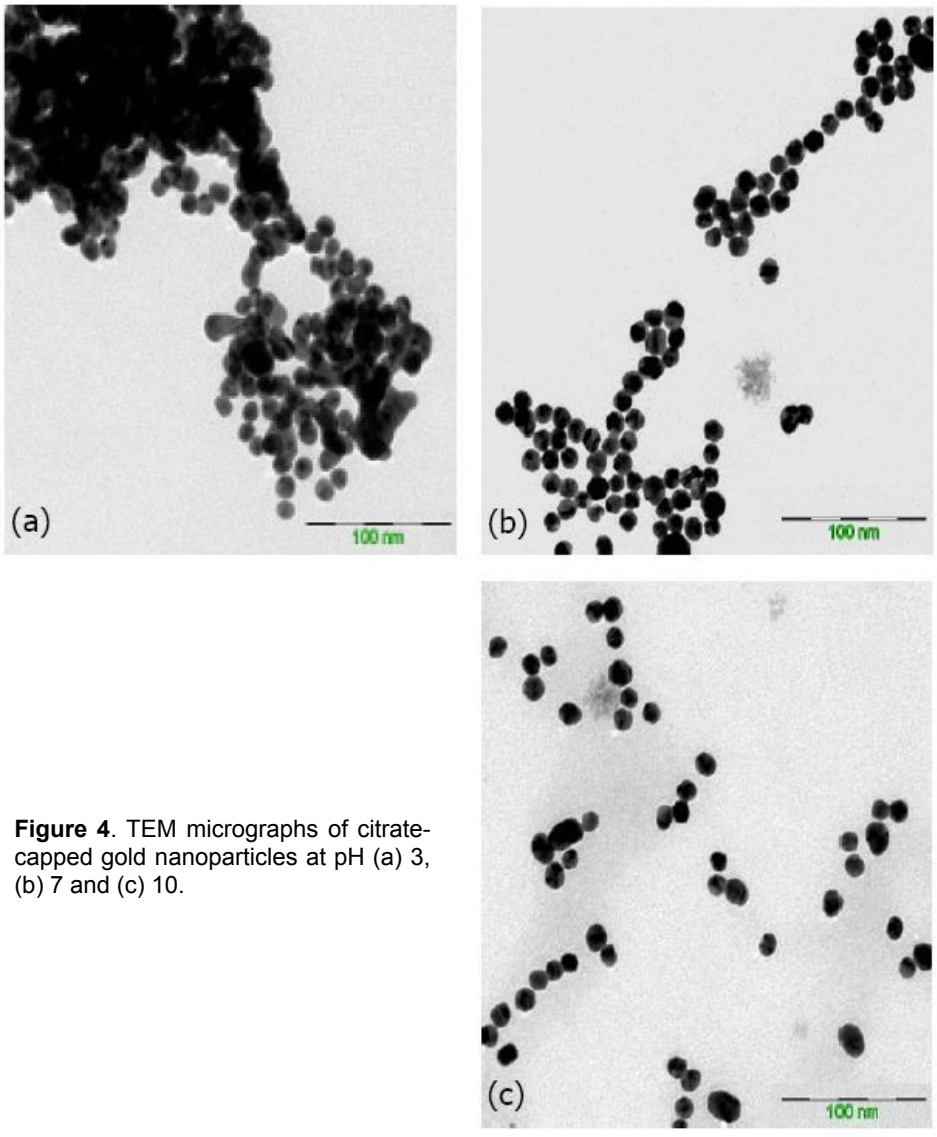

Figure 4. TEM micrographs of citrate-capped gold nanoparticles at pH (a) 3, (b) 7 and (c) 10.

RESULTS AND DISCUSSION

Characterization of Citrate-Capped Gold Nanoparticles

The citrate-capped gold nanoparticles were synthesized by chemical reduction using $HAuCl_4$ as the precursor salt and citrate as the reducing agent. The pH value of the synthesized citrate-capped gold nanoparticles was measured to be around 6.0-6.1. The UV-Vis absorption spectrum of the citrate-capped gold nanoparticles is shown in Figure 1. The absorption band centered at ~520 nm is characteristic of gold nanoparticles and is due to the surface plasmon resonance absorption which gives rise to the gold nanoparticles' distinctive red color (Patungwasa and Hodak 2007). TEM was used to measure the particle size of the citrate-capped gold nanoparticles. Figure 2

shows the TEM micrographs of the citrate-capped gold nanoparticles taken at 40000x magnification. As can be seen from the micrographs, the gold nanoparticles are mostly spherical in shape. Further analysis confirmed that the nanoparticles exhibited an average of 12.2 nm diameter size with a standard deviation of 1.65.

Effect of pH

Variation in the pH of the gold nanoparticles solution was detected to have an effect on the optical property of the gold nanoparticles. Adjustment of the pH value of the gold nanoparticle solution from pH 4 to 10 did not show any change in its wine red coloration. This also indicates the stability of the disperse state of the gold nanoparticles in this pH value range. However at pH value 3, the color already became purple which is an indication that slight aggregation had taken place. And further adjustment to a pH value below 3 already caused the gold nanoparticles solution to turn blue, which showed that the gold nanoparticles had already aggregated.

The color distinction with pH was also reflected in the UV-Vis spectra. Figure 3 shows the LSPR band of the gold nanoparticles with the addition of HCl or NaOH. For the addition of HCl, there is no observable shift in the LSPR band peak position until the pH is around 4, indicating no aggregation effect. However, as the pH approaches 3, a sign of aggregation becomes apparent. The aggregation is indicated by the appearance of a shoulder peak which is approximately centered at 610 nm. This may be the result of surface charge neutralization of the particles caused by the addition of HCl (Basu et al. 2007). For the addition of NaOH, no indication of aggregation was observed even at pH values above 10.

The aggregation of gold nanoparticles at pH 3 was further confirmed by TEM analysis. TEM micrographs of gold nanoparticles solution at pH 3, 7 and 10 are shown in

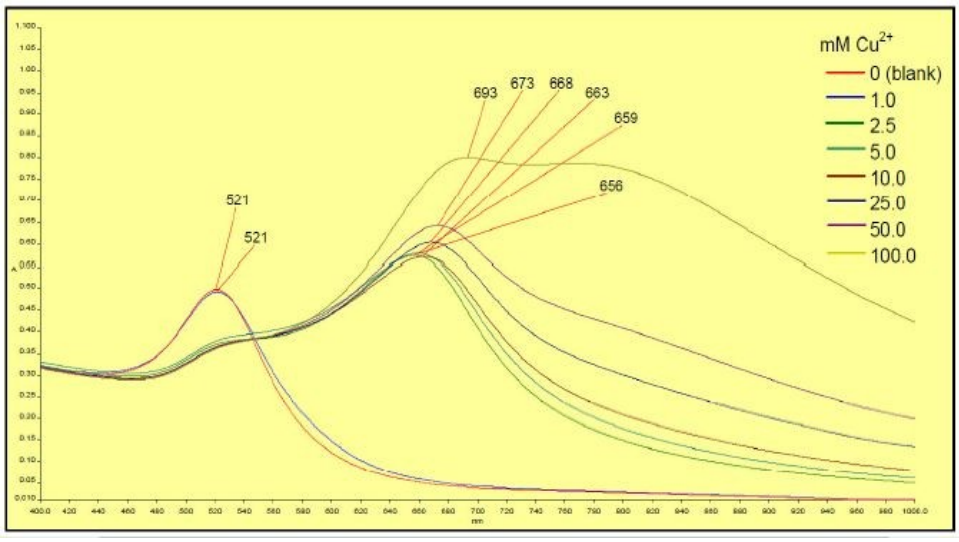

Figure 5. UV-Vis spectra of gold nanoparticles with varying concentrations of Cu^{2+}

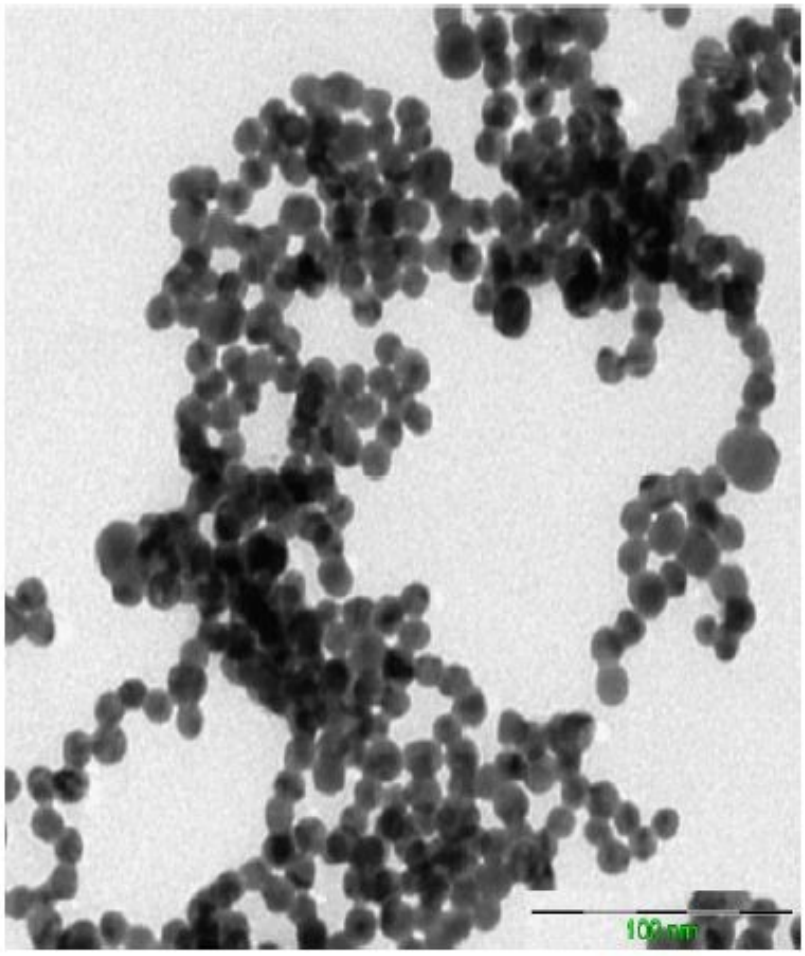

Figure 6. TEM micrographs of aggregated gold nanoparticles due to the presence of 2.5 mM Cu^{2+}.

Figure 4. For pH 7 and 10 (Figures 4b and 4c), the particles are still dispersed with no signs of aggregation observed and the mean particle diameter was determined to be 12.7 ± 2.6 and 12.0 ± 1.9, respectively. For pH 3 (Figure 4a), it is evident that aggregation had taken place due to closer confinement of the particles. This observation also coincides with the UV-Vis spectrum and visual analysis of the color of the gold nanoparticles solution at pH 3. Although most of the gold nanoparticles still mainly consist of 12 nm diameter size particles at this pH, the particles already have a broader size distribution in the range of 7-28 nm, compared to those at pH 7 and 10 with a size distribution range of only 9-18 nm.

Effect of Copper(II) Ions

Copper(II) ions were noted to affect the stability of citrate-capped gold nanoparticles in aqueous solution. Addition of 2.5mM to 100mM Cu^{2+} showed a red-to-blue change in color; only the addition of 1.0mM Cu^{2+} did not exhibit any change in color, suggesting that no aggregation had taken place. These observations were also confirmed by the UV-Vis absorption spectra taken after the addition of the different concentrations of Cu^{2+} (Figure 5). The absorption spectra also did not show any observable change with the addition of 1.0 mM Cu^{2+}, while with the addition of 2.5mM to 100mM noticeable red shifts were observed with increasing absorption peak band intensities as the concentration was increased.

The TEM micrographs of the gold nanoparticles solution after addition of Cu^{2+} (Figure 6) clearly indicate the formation of aggregated gold nanoparticles. This fact strongly supports the notion that the interparticle distance is reduced. When the interparticle distance in the aggregates decreases to less than about the average particle diameter, the electric dipole–dipole interaction and coupling between the plasmons of neighboring particles in the aggregates result in the red shift of the absorption band (Mocanu et al. 2009).

Colorimetric Assay of Copper(II) Ions Based on Gold Nanoparticles Aggregation

Copper(II) ions can be quantitated based on its aggregation effects on gold nanoparticles. The aggregation can be monitored visually through the change in color and spectrophotometrically through the change in the absorption spectra. It was noted that with increasing concentration of Cu^{2+}, the surface plasmon band originally centered at ~520 nm decreases dramatically as a new absorption band between 670 nm to 700 nm progresses. Inspection of the spectra shows maximum divergence at 700 nm. At this wavelength, high sensitivity can therefore be achieved.

The aggregation of the gold nanoparticles in the presence of Cu^{2+} was found to vary with time. Upon addition of the Cu^{2+} to the gold nanoparticles solution, abrupt color changes from red to blue were observed. Time-dependence monitoring of the aggregation process of gold nanoparticles in the presence of different Cu^{2+} concentrations showed that after 360 seconds the absorbance changes were already very minimal. This indicates the formation of stable aggregates and therefore ensures good reproducibility of the absorbance readings after this time duration. For Cu^{2+} concentrations of 10mM and 25mM, relative standard deviation (r.s.d.) values of 5.36% and 3.70%, respectively, for 6 trials were obtained.

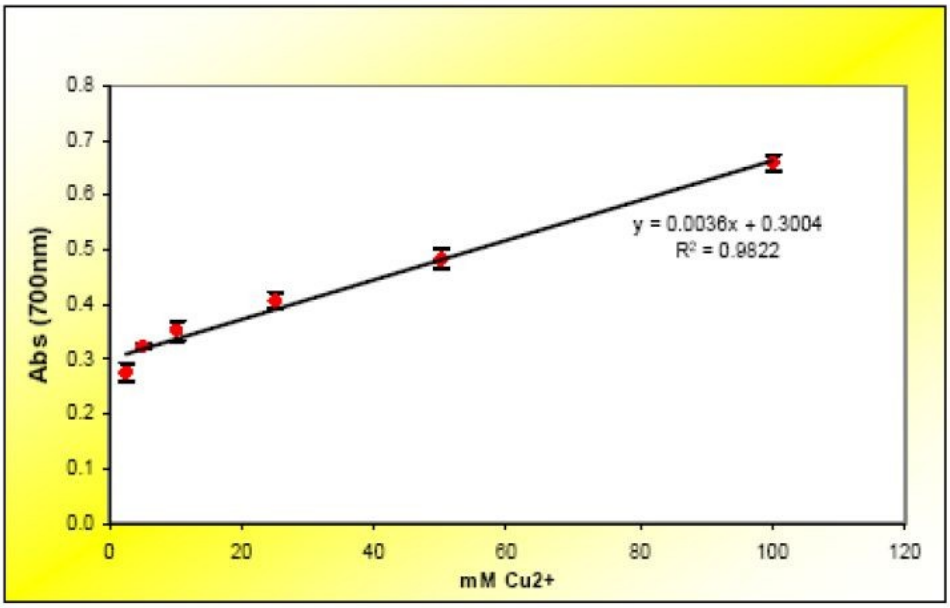

Figure 7. Calibration curve for the determination of Cu^{2+} at optimum parameters

The pH of the gold nanoparticles solution was also found to vary with the absorbance readings of the nanoparticles towards Cu^{2+}. As mentioned previously in section 3.2, stability of gold nanoparticles was affected by the pH of its surrounding medium. Thus, variation in the pH value of its medium will affect its sensitivity and response to Cu^{2+}. The pH value of the gold nanoparticles solutions was then varied before the addition of Cu^{2+}. Upon assessment of the plot of the absorbance versus the Cu^{2+} concentrations at different pH values (from pH 4 to pH 10), the best linear plot was obtained at pH 4.

At these optimum parameters

(i.e., wavelength, reaction time, and pH), the calibration curve displayed a sensitivity of 0.0036 A.U./mM and a linearity of 0.9822 r^2 (Figure 7). The calculated detection limit for the determination method is 5.0 mM.

CONCLUSION

Citrate-capped gold nanoparticles were synthesized in aqueous medium via a chemical reduction method. In this method, citrate served the dual purpose of being the reducing agent and the stabilizer. The citrate-capped gold nanoparticles solution displayed a wine red color and characterization through UV-Vis spectroscopy showed a characteristic LSPR band at 520 nm. The presence of spherical gold nanoparticles with average particle diameter size of 12.2 nm ± 1.65 was confirmed by TEM analysis. Gold nanoparticles aggregate upon disruption of the stabilizer. A colorimetric method for the determination of Cu^{2+} was demonstrated based on the aggregation of citrate-capped gold nanoparticles. Cu^{2+} assay calibration curves were constructed under optimum parameters (wavelength, reaction time, and pH). The calibration curve for the Cu^{2+} determination has a linearity value of 0.9822 r^2 and sensitivity of 0.0036 A.U./mM. Good reproducibility was also observed with a computed relative standard deviation values of 1.56-6.15% (n=6) for the linear range from 2.5mM to 100mM. The limit of detection for the calibration curve is 5.0 mM.

ACKNOWLEDGMENT

The authors would like to acknowledge the National Kidney and Transplant Institute for the Transmission Electron Microscopy analysis. The University of Santo Tomas Graduate School is also duly acknowledged for their cooperation and assistance in the accomplishment of the study.

CONFLICT OF INTEREST

There is no conflict of interest in this study.

CONTRIBUTION OF INDIVIDUAL AUTHORS

Alan Rodelle M. Salcedo conducted all wet laboratory experiments, including the synthesis and characterization of the gold nanoparticles, and optimization of parameters for the Cu(II) ion determination. Fortunato B. Sevilla, III supervised all experiments and data treatment and analyses.

REFERENCES

Aryal S, Bahadur RKC, Khil MS, Dharmaraj N, Kim HY. Radical scavenger for the stabilization of gold nanoparticles. Materials Letters 2007; 61:4225–4230.

Aslan K, Lakowicz JR, Geddes CD. Nanogold-plasmon-resonance-based glucose sensing. Analytical Biochemistry 2004; 330:145-155.

Basu S, Ghosh SK, Kundu S, Panigrahi S, Praharaj S, Pande S, Jana S, Pal T. Biomolecule Induced Nanoparticle Aggregation: Effect of Particle Size on Interparticle Coupling. Journal of Colloid and Interface Science 2007; 313:724-734.

Brewer SH, Glomm WR, Johnson MC, Knag MK, Franzen S. Probing BSA binding to citrate-coated gold nanoparticles and surfaces. Langmuir 2005; 21:9303-9307.

Huang C-C, Chang H-T. Selective gold-nanoparticle-based "turn-on" fluorescent sensors for detection of mercury(II) in aqueous solution. Anal Chem 2006; 78(24): 8332-8336.

Kattumuri V, Chandrasekhar M, Guha S, Raghuraman K, Katti KV, Ghosh K, Patel RJ. Agarose-stabilized gold nanoparticles for surface-enhanced Raman spectroscopic detection of DNA nucleosides. Applied Physics Letters 2006; 88:153114.

Kim Y, Johnson RC, Hupp JT. Gold Nanoparticle-Based Sensing of "Spectroscopically Silent" Heavy Metal Ions. Nano Letters 2001; 1(4):165-167.

Kubo Y, Uchida S, Kemmochib Y, Okubob T. Isothiouronium-modified gold nanoparticles capable of colorimetric sensing of oxoanions in aqueous MeOH solution. Tetrahedron Letters 2005; 46:4369–4372.

Lee J-S, Han MS, Mirkin CA. Colorimetric Detection of Mercuric Ion (Hg^{2+}) in Aqueous Media using DNA-Functionalized Gold Nanoparticles. Angew Chem Int Ed 2007; 46:4093-4096.

Liang R-Q, Tan C-Y, Ruan K-C. Colorimetric detection of protein microarrays based on nanogold probe coupled with silver enhancement. Journal of Immunological Methods 2004; 285:157–160.

Liu J, Lu Y. A Colorimetric Lead Biosensor Using DNAzyme-Directed Assembly of Gold Nanoparticles. J Am Chem Soc 2003; 125:6642-6643.

Luo Y. Size-controlled preparation of polyelectrolyte-protected gold nanoparticles by natural sunlight radiation. Materials Letters 2007; 61:2164–2166.

Mocanu A, Cernica I, Tomoaia G, Bobos L-D, Horovitz O, Tomoaia-Cotisel M. Self-Assembly Characteristics of Gold Nanoparticles in the Presence of Cysteine. Colloids and Surfaces A: Physiochemical and Engineering Aspects 2009; 338(1-3):93-101.

Patungwasa W, Hodak JH. pH tunable morphology of the gold nanoparticles produced by citrate reduction. Materials Chemistry and Physics 2007; 108:45-54.

Rho S, Kim SJ, Lee SC, Chang JH, Kang H-G, Choi J. Colorimetric Detection of ssDNA in a Solution. Current Applied Physics 2008; 9(2):534-537.

Sarkar T, Roy S, Bhattacharya J, Bhattacharya D, Mitra CK, Dasgupta AKr. Thermal hysteresis of some important physical properties of nanoparticles. Journal of Colloid and Interface Science 2008; 327:224–232

Simonian AL, Good TA, Wang S-S, Wild JR. Nanoparticle-based optical biosensors for the direct detection of organophosphate chemical warfare agents and pesticides. Analytica Chimica Acta 2005; 534:69–77.

Sugunan,A, Dutta J. Novel Synthesis of Gold Nanoparticles in Aqueous Media. Materials Research Society Symposium Proceedings 2005; 901:257-262.

Sugunan A, Thanachayanont C, Dutta J, Hilborn JG. Heavy-metal ion sensor using chitosan-capped gold nanoparticles. Science and Technology of Advanced Materials 2005; 6:335-340.

Sun Y, Bai Y, Yang W, Sun C. Controlled multilayer films of sulfonate-capped gold nanoparticles/thionine used for construction of a reagentless bienzymatic glucose biosensor. Electrochimica Acta 2007; 52:7352–7361.

Wang Z, Ma L. Gold Nanoparticle Probes. Coordination Chemistry Reviews 2009; 253(11-12):1607-1618.

Watanabe S, Seguchi H, Yoshida K, Kifune K, Tadakib T, Shiozakic H. Colorimetric detection of fluoride ion in an aqueous solution using a thioglucose-capped gold nanoparticle. Tetrahedron Letters 2005; 46:8827–8829.

Wu Z-S, Zhang S-B, Guo M-M, Chen C-R, Shen G-L, Yu R-Q. Homogeneous, unmodified gold nanoparticle-based colorimetric assay of hydrogen peroxide. Analytica Chimica Acta 2007; 584:122–128.

Ye J, Bonroy K, Nelis D, Frederix F, D'Haen J, Maes G, Borghs G. Enhanced localized surface plasmon resonance sensing on three-dimensional gold nanoparticles assemblies. Colloids and Surfaces A: Physicochem Eng Aspects 2008; 321:313–317

Yoosaf K, Ipe BI, Suresh CH, Thomas KG. In Situ Synthesis of Metal Nanoparticles and Selective Naked-Eye Detection of Lead Ions from Aqueous Media. J Phys Chem C 2007; 111(34):12839-12847.